# Accelerating monoenergetic protons from ultrathin foils by flat-top laser pulses in the directed-Coulomb-explosion regime

S. S. Bulanov,[1,2] A. Brantov,[3] V. Yu. Bychenkov,[3] V. Chvykov,[1] G. Kalinchenko,[1] T. Matsuoka,[1] P. Rousseau,[1] S. Reed,[1] V. Yanovsky,[1] D. W. Litzenberg,[4] K. Krushelnick,[1] and A. Maksimchuk[1]

[1]*FOCUS Center and Center for Ultrafast Optical Science, University of Michigan, Ann Arbor, Michigan 48109, USA*

[2]*Institute of Theoretical and Experimental Physics, Moscow 117218, Russia*

[3]*P. N. Lebedev Physics Institute, Russian Academy of Sciences, Moscow 119991, Russia*

[4]*Department of Radiation Oncology, University of Michigan, Ann Arbor, Michigan 48109, USA*

(Received 14 September 2007; revised manuscript received 12 May 2008; published 22 August 2008)

We consider the effect of laser beam shaping on proton acceleration in the interaction of a tightly focused pulse with ultrathin double-layer solid targets in the regime of directed Coulomb explosion. In this regime, the heavy ions of the front layer are forced by the laser to expand predominantly in the direction of the pulse propagation, forming a moving longitudinal charge separation electric field, thus increasing the effectiveness of acceleration of second-layer protons. The utilization of beam shaping, namely, the use of flat-top beams, leads to more efficient proton acceleration due to the increase of the longitudinal field.

DOI: 10.1103/PhysRevE.78.026412 PACS number(s): 52.38.Kd, 29.25.Ni, 52.65.Rr, 41.85.Ct

## I. INTRODUCTION

The recent development of compact laser systems capable of generating repetitive ultrashort pulses in the multiterawatt and even petawatt power range make charged particle acceleration from laser-matter interaction one of the most important potential applications of these systems. The generation of ion beams with a maximum energy of a few to tens of MeV has been observed in many experiments on laser pulse interaction with solid targets [1]. Two- and three-dimensional particle-in-cell computer simulations show that by optimizing the parameters of the laser pulse and the target it is possible to obtain effective ion acceleration [2,3], which can be utilized in hadron therapy [4–6], fusion ignition [7–9], and proton radiography [10]. The highest proton energies were experimentally achieved with single-shot multijoule picosecond pulse duration Nd:glass lasers. However, ultrashort-pulse (tens of femtoseconds) Ti:sapphire lasers may be more advantageous for applications and fundamental studies. This is due to the fact that they have much higher repetition rates that is an important requirement for proton therapy, isotope production, and injection of charged particles into accelerators [10]. Such lasers also enable ultrahigh intensities [11,12] that allow for the investigation of new regimes of laser-matter interactions [13].

Several regimes are considered for ion acceleration from foils: (i) target normal sheath acceleration (TNSA) [14], through the sheath of hot electrons produced at the front of the target, (ii) Coulomb explosion [15], through the charge separation electric field generated by the exploding ion core after the evacuation of all the electrons, and (iii) the laser piston regime [16], through the electromagnetic wave pressure. In recently proposed schemes the TNSA is coupled to the energy conversion from an expanding electron cloud to the expanding ion cloud under the action of burning through the foil laser pulse [17]. In another scheme the Coulomb explosion is optimized by injecting a proton bunch into the longitudinal field [18].

In this paper, we report on a mechanism of high-energy ion acceleration in the interaction of prepulse-free high-intensity laser with double layer [4,19,20] ultrathin foils, namely, on the regime of directed Coulomb explosion (DCE). In this regime a high-intensity laser pulse not only expels electrons from the irradiated area of the foil but also accelerates the remaining ion core, which begins to move in the direction of pulse propagation. Then the ion core experiences a Coulomb explosion due to the excess of positive charges, transforming into a cloud expanding predominantly in the laser propagation direction with a strong one-dimensional (1D) longitudinal electric field moving ahead of it, which accelerates protons from the second layer. Thus this regime is an efficient combination of the radiation pressure [16] and Coulomb explosion effects [15]. As the expansion evolves, 3D effects become significant resulting in highly reduced efficiency of ion acceleration [21].

We suggest using flat-top laser beams to enhance proton acceleration in the DCE regime and to achieve generation of monoenergetic proton beams with high energy and small energy spread. Such super-Gaussian beams, having the same energy as Gaussian ones, evacuate electrons from a larger area on the foil, generating stronger longitudinal field and thus more energetic protons.

The paper is organized as follows. The theoretical description of DCE along with the estimate of maximum proton energy is presented in Sec. II. The utilization of flat-top beams and the resulting effect on the proton maximum energy are discussed in Sec. III. The results of 2D particle-in-cell (PIC) simulations of proton acceleration from ultrathin double-layer foils by laser pulses with different profiles are presented in Sec. IV. We conclude in Sec. V.

## II. DIRECTED COULOMB EXPLOSION

For a very thin target, laser light just evacuates the electrons from the focal spot and transmits through the foil without pushing it and proton acceleration can only be due to Coulomb explosion [15]. When the foil is thicker the light is reflected. The foil is then accelerated by the radiation pressure [16]. In contrast to the previously discussed schemes

 

[2,14–16] we consider a preplasma-free laser interaction with double-layer [4,19,20] aluminum-hydrogen (heavy ions–light ions) foils of such thicknesses that a regime of acceleration comes into play, where both Coulomb explosion and radiation pressure contribute to proton acceleration. Even if electrons of the foil are not completely evacuated from the focal spot and the effect of Coulomb explosion is reduced, radiation pressure can compensate for this, providing some proton energy increase. The laser pulse not only expels electrons from the irradiated area but also accelerates the remaining ion core, which begins to move in the direction of pulse propagation. Then the ion core experiences a Coulomb explosion due to the excess of positive charges, transforming into a cloud expanding predominantly in the laser propagation direction with a strong longitudinal electric field moving ahead of it. Let us estimate the maximum proton energy that can be gained by means of the mechanism described above. First, we calculate the momentum of heavy ions.

The radiation pressure is the sum of incident, transmitted, and reflected electromagnetic wave momentum fluxes, $P=(E'^2/4\pi)(1+|R|^2-|T|^2)$. Here $R$ and $T$ are the amplitudes of the reflected and transmitted waves, respectively, in the instantaneous reference frame, where the foil is at rest. In the moving (laboratory) frame the laser field is $E'$ $(E)$ and its frequency is $\omega'$ $(\omega)$. Taking into account energy conservation, $|R|^2+|T|^2=1$, we obtain for the radiation pressure in terms of laboratory frame variables

$$P=(E^2/2\pi)(\omega/\omega')|R|^2.$$

In fact the foil reference frame is not inertial since the foil is accelerated. Hence, the electromagnetic wave frequency $\omega'$ decreases with time in this frame [22]. Nevertheless, we can assume that the acceleration is relatively small and thus $(\omega'/\omega)=(c-V)/(c+V)$, where $V=dx/dt$ is the foil instantaneous velocity.

The equation of foil motion reads as follows [16]:

$$\frac{dp}{dt}=\frac{E^2[t-x(t)/c]}{2\pi n_e L}|R|^2\frac{\sqrt{m_i^2c^2+p^2}-p}{\sqrt{m_i^2c^2+p^2}+p}, \tag{1}$$

where $L$ is the foil thickness, $n_e$ is the electron density of the foil, $p$ is the momentum of heavy ions representing the foil, and $m_i$ is the heavy ion mass. Following the approach of Ref. [16] we write down the ion momentum in terms of the dimensionless variable $\psi=\int_{-\infty}^{t-x(t)/c}[E^2(\zeta)/4\pi n_e L m_i c]d\zeta$, which can be interpreted as the normalized energy of the portion of the laser pulse that has been interacting with the moving foil by time $t$; $\max\{\psi\}=W/N_i m_i c^2$, where $W$ is the laser pulse energy and $N_i=\pi\rho^2 L n_i$ ($\rho$ is the focal spot radius and $n_i$ is the heavy ion density) is the total number of heavy ions in the accelerated portion of the foil:

$$p/m_i c=\frac{(h_0+2\kappa\psi)^2-1}{2(h_0+2\kappa\psi)}, \tag{2}$$

where $h_0=p_0/m_i c+(1+p_0^2/m_i^2c^2)^{1/2}$, $\kappa=(1/\psi)\int_0^{\psi}|R(\omega')|d\psi$, and $p_0$ is the initial momentum of heavy ions. The maximum value of the momentum gained by the foil that was initially at rest $(p_0=0)$ is

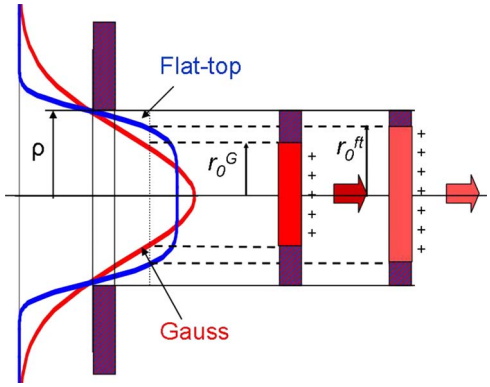


FIG. 1. (Color online) Principal scheme of foil fraction acceleration by Gaussian (radius of the area with all electrons expelled is $r_0^G$) and flat-top beams (radius of the area with all electrons expelled is $r_0^{ft}$).

$$\max\{p/m_i c\}=\frac{(1+\kappa W/N_i m_i c^2)^2-1}{2(1+2\kappa W/N_i m_i c^2)}. \tag{3}$$

In the nonrelativistic case, $\max\{\psi\}\ll 1$, and Eq. (3) reads $\max\{p/m_i c\}=2\kappa W/N_i m_i c^2$.

As mentioned above, the moving heavy ions generate a longitudinal charge separation electric field, which accelerates protons. In the reference frame, where the foil is at rest, the energy of protons can be estimated as [15,23]

$$\mathcal{E}'=2\pi^2 m_e c^2\frac{n_e}{n_{\rm cr}}\frac{Lr_0}{\lambda^2}, \tag{4}$$

where $r_0$ is the radius of a spot with all the electrons expelled (see Fig. 1), $n_{\rm cr}$ is the critical plasma density, and $\lambda$ is the laser wavelength. Here we assumed that the protons are accelerated near the surface of a charged disk and the acceleration distance is of the order of $r_0$.

In the laboratory frame these protons will have the following kinetic energy:

$$\mathcal{E}=\frac{\mathcal{E}'+Vp'}{\sqrt{1-V^2/c^2}}=(\mathcal{E}'+m_p c^2)\sqrt{1+(p/m_i c)^2}+(p/m_i c)\sqrt{(\mathcal{E}'+m_p c^2)^2-m_p^2c^4}-m_p c^2, \tag{5}$$

where $m_p$ is the proton mass. For $p\ll m_i c$ and $\mathcal{E}'\ll m_p c^2$,

$$\mathcal{E}=\mathcal{E}'+(p/m_i c)\sqrt{2\mathcal{E}' m_p c^2}. \tag{6}$$

In this case the energy gain due to the radiation pressure is added to the energy acquired in the static charge separation field. For a 500 TW laser pulse interacting with a 0.1λ-thick, $n_e=400n_{\rm cr}$ aluminum foil with a layer of hydrogen on the back, this formula gives a 100% energy increase over the value acquired in the static charge separation field.

In the ultrarelativistic case, $p\gg m_i c$, the radiation pressure plays the main role:

$$\mathcal{E} = \begin{cases} (p/m_i c)(m_p c^2 + \sqrt{2\mathcal{E}' m_p c^2}), & \mathcal{E}' \ll m_p c^2, \\ 2(p/m_i c)\mathcal{E}', & \mathcal{E}' \gg m_p c^2. \end{cases} \quad (7)$$

However in both cases the Coulomb explosion gives a significant contribution to the proton final energy. Let us compare these two cases from the point of view of maximizing the proton energy for given laser pulse energy. The radiation pressure effect is inversely proportional to the number of ions in the focal spot and thus to the focal spot radius squared, i.e., $p=A/\rho^2$. The energy gain in the longitudinal charge separation field is proportional to the focal spot radius, i.e., $\mathcal{E}'=B\rho$ (here we assumed that in the ultrarelativistic case the electrons are completely evacuated from the focal spot). Then the energy in Eq. (5) can be written in the form $\mathcal{E}(\rho) \sim A[1/\rho^2 + B/\rho + \sqrt{(B/\rho^2)^2 + 2B/\rho^3}]$. This function tends to zero as $\rho \to \infty$ ($\mathcal{E}' \gg m_p c^2$) and it tends to infinity as $\rho \to 0$ ($\mathcal{E}' \ll m_p c^2$). So the case $p \gg m_i c$ and $\mathcal{E}' \ll m_p c^2$ is more beneficial for maximizing the proton energy. However, the focal spot is limited by diffraction, $\rho \sim 0.5\lambda$, and the proton energy reaches its maximum at this value of $\rho$. For a 1 kJ [24] pulse, focused to the diffraction limit, interacting with a $0.1\lambda$-thick, $n_e=400n_{\rm cr}$ aluminum foil with a layer of hydrogen on the back, the total energy is $\mathcal{E}=18m_p c^2$, while the energy gain due to Coulomb explosion is $\mathcal{E}'=0.2m_p c^2$, and $p=10m_i c$.

## III. FLAT-TOP BEAMS

The use of super-Gaussian beams [25] can lead to proton beam quality improvement, i.e., maximum energy increase and reduction of energy spread above the values generated by the conventional Gaussian beams for the same laser pulse energy. This is due to the fact that flat-top beams evacuate electrons from a larger area on the part of the foil accelerated by the radiation pressure (see Fig. 1), and are more efficient in preventing the radial return of electrons because of higher radial ponderomotive force. Super-Gaussian beams generate a stronger longitudinal electric field and flatten the charge separation electric field in the radial direction leading to a more monoenergetic proton beam.

In order to estimate the dependence of the maximum energy of protons on the beam shape, we calculate the energy gain in the quasistatic electric field along the $x$ axis which is due to charge separation. The magnitude of the longitudinal electric field depends on the charge distribution in the part of the foil accelerated by the radiation pressure during and after the interaction with the laser pulse. The charge distribution itself in turn depends on the laser beam shape. In order to study this dependence we use laser beams with the same energy but different beam profiles (for the Gaussian pulse we use Gaussian transverse and longitudinal profiles; for the flat-top pulse we use Gaussian longitudinal and flat-top transverse profiles). Beams with different shapes and the same energy accelerate parts of the foil with the same radius $\rho$ (Fig. 1). That is why the laser beam shaping will affect only $\mathcal{E}'$ in Eq. (5). We assume that the transverse charge distribution is axially symmetric and the longitudinal one is uniform:

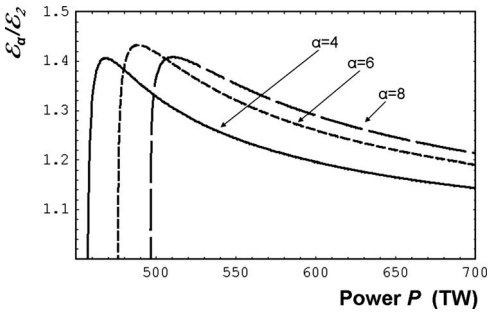


FIG. 2. Dependencies of the ratio of maximum proton energy gained in the longitudinal field generated by a laser pulse with super-Gaussian beam profile and the one gained in the field generated by a pulse with Gaussian profile on laser pulse power for different beam profiles ($\alpha=4,6$, and 8); $n_e=400n_{\rm cr}$, $l_{\rm Al}=0.1\lambda$ (2D case, presented to compare with PIC simulation results)

$$E \sim \int_0^{r_0 H(\rho-r_0)+\rho H(r_0-\rho)} \frac{n_e}{n_{\rm cr}} \frac{\tilde{x} r\, dr}{(\tilde{x}^2+r^2)^{3/2}} + H(\rho - r_0) \int_{r_0}^{\rho} \frac{n_e(r)}{n_{\rm cr}} \frac{\tilde{x} r\, dr}{(\tilde{x}^2+r^2)^{3/2}}, \quad (8)$$

where $H(x)$ is the Heaviside step function: $H(x)=0$ for $x<0$ and $H(x)=1$ for $x>0$. The first term in Eq. (8) represents the electric field generated by an area with radius $r_0$ where all the electrons are expelled. The second term represents the electric field generated by the area outside the radius $r_0$. The Heaviside step functions are needed to ensure that in the case of $r_0 \geqslant \rho$ (i.e., when all the electrons are expelled from the accelerated part of the foil) only the first term in Eq. (8) survives with the limits of integration from 0 to $\rho$. Here $\tilde{x}$ is the distance from the foil along the $x$ axis. The amplitude of the vector potential, $a(r)$, necessary for the fraction of accelerated electrons $dN=n_e L\, dS$ ($dS$ is the element of the foil surface) to escape the attraction of the remaining ions is

$$a(r) = \pi \frac{n_e(r)}{n_{\rm cr}} \frac{L}{\lambda}. \quad (9)$$

If this fraction $dN$ for any $r$ equals the total number of electrons in the volume $L\, dS$, then the equation $a(r_0) = \pi(n_e/n_{\rm cr})(L/\lambda)$ has a solution. If we assume that $a(r) = a_\alpha \exp[-(r/\rho)^\alpha]$, $\alpha=2$ for Gaussian, $\alpha=4,6,8,\ldots,2k$ for a flat-top (or super-Gaussian) beam profile, then

$$r_0 = \rho \left[ \ln\left( \frac{a_\alpha n_{\rm cr} \lambda}{\pi n_e L} \right) \right]^{1/\alpha}. \quad (10)$$

Here the amplitudes $a_\alpha$ are obtained by fixing the laser pulse energy and calculating the maximum value of the electric field for each beam profile. The dependence of the maximum proton energy ($\mathcal{E}'=\int_0^{r_0} E\, dx$) normalized to the maximum energy gained in the Gaussian pulse on laser pulse power is presented in Fig. 2. Even if the ponderomotive force, which leads to higher positive charge in the focal spot, is not taken into account, the protons gain up to 40% more energy in the charge separation field generated by super-Gaussian pulses for the same value of laser energy, because super-Gaussian

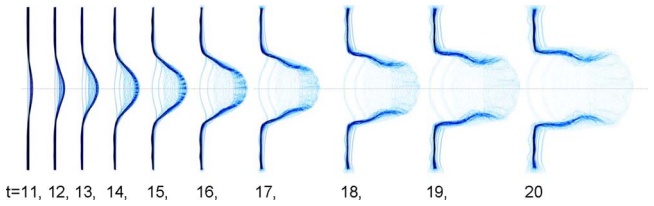


FIG. 3. (Color online) Evolution of heavy ion density (from cycle 11 to cycle 20) in the 500 TW laser pulse interaction with a 0.1λ thick aluminum foil.

pulses expel the electrons from a larger area. This effect depends on the matching of the laser pulse power to the thickness of the foil. It manifests itself most strongly when the peak of the pulse is able to penetrate the foil but not able to completely evacuate electrons from the focal spot.

## IV. 2D PIC RESULTS

In our numerical model with the 2D PIC code REMP (relativistic electromagnetic particle) mesh code based on the particle-in-cell method [26], the acceleration of ions is studied in a high-intensity laser interaction with an ultrathin double-layer aluminum-hydrogen foil. The grid mesh size is $\lambda/200$, space and time scales are given in units of λ and $2\pi/\omega$, respectively, and the simulation box size is $20\lambda \times 10\lambda$. The 500 TW (peak intensity of $2.7\times10^{22}$ W/cm$^2$) 30 fs duration laser pulse, introduced at the left boundary and propagating along the $x$ axis from left to right, is tightly focused [$f/D=1.5$, spot size is 1λ full width at half maximum (FWHM)] at the foil, which is placed at the distance of $f=3.33\lambda$ from the left boundary. The pulse is linearly polarized along the $z$ axis, perpendicular to the simulation plane ($xy$). Two types of pulses were used: first, a pulse with Gaussian transverse and longitudinal profile, and, second, one with flat-top transverse ($\alpha=6$) and Gaussian longitudinal profile. The target is composed of two layers: high-$Z$, fully ionized aluminum $Al^{13+}$ with an electron density of $400n_{cr}$, thickness $L_{Al}=0.1\lambda$, and diameter $D_{Al}=9\lambda$; and low-$Z$ layer, ionized hydrogen ($H^+$, $n_H=30n_{cr}$), with a thickness $L_H=0.05\lambda$ and diameter $D_H=1.0\lambda$. This geometry is chosen to exclude from the analysis the low-energy protons, as well as to clarify the difference between the Gaussian pulse and flat-top pulse cases with the same total energy. As mentioned above, the material of the foil is assumed to be fully ionized. This is justified since the intensity needed to fully ionize aluminum is approximately $6\times10^{20}$ W/cm$^2$, while we use in simulations the intensity at least one order of magnitude larger. So the foil will become fully ionized well before the arrival of the pulse peak and can be modeled as a double-layer slab of the overdense plasma.

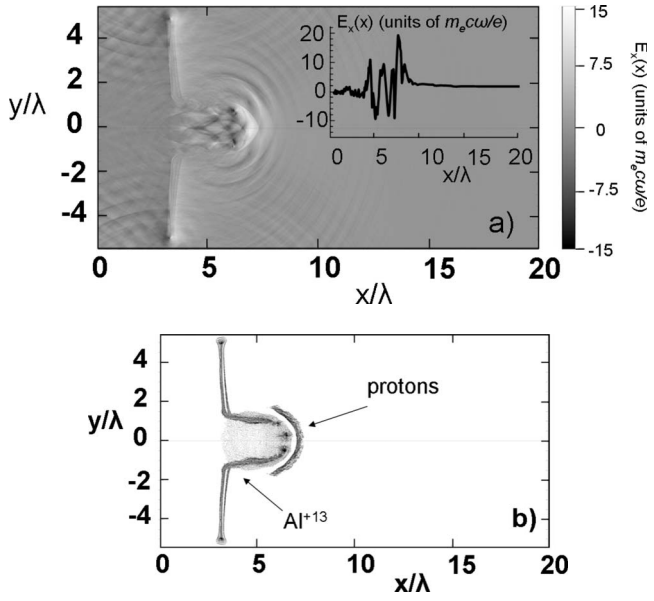


FIG. 4. Interaction of a 500 TW laser pulse ($f/D=1.5$) with ultrathin double-layer foil. (a) The dependence of the electric longitudinal field strength on spatial coordinates at $t=23$, the inset represents the longitudinal field behavior along $y=0$. (b) Ion density distribution at $t=23$.

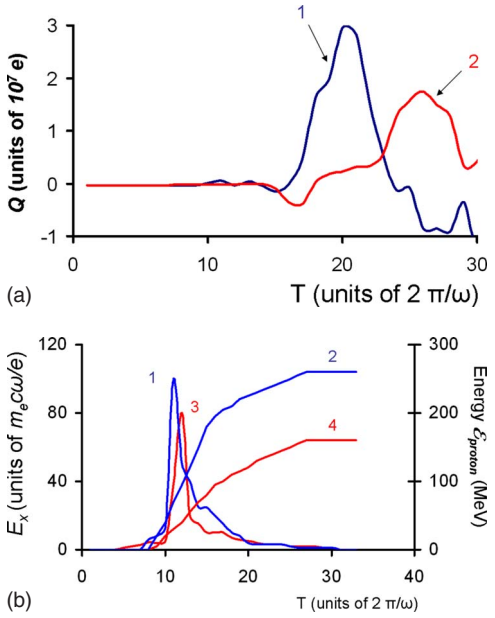


FIG. 5. (Color online) Interaction of a focused ($f/D=1.5$) 500 TW laser pulse with a 0.1λ-thick aluminum foil with 0.05λ-thick hydrogen second layer. (a) The dependence of the total charge (1 for flat-top and 2 for Gaussian beams) in the area $0<x<20$, $-1.5<y<1.5$ on time. (b) The dependence of maximum values of the accelerating longitudinal electric field (1 for flat-top and 3 for Gaussian beams) and proton energy (2 for flat-top and 4 for Gaussian beams) on time. Charge is measured in units of electron charge, time in wave periods, proton energy in MeV, and electric field in units of $m_ec\omega/e$.

In order to justify our assumption made in Sec. II, that, at first, the foil is accelerated by radiation pressure as a whole and then experiences Coulomb explosion, we present a set of figures illustrating the evolution of heavy ion density in Fig. 3. One can see that, indeed, initially the heavy ions are accelerated by the radiation pressure and only after 15 cycles do they experience Coulomb explosion. Thus as a result of laser pulse interaction with heavy ion layer the latter is transformed into a cloud expanding predominantly in the direc-

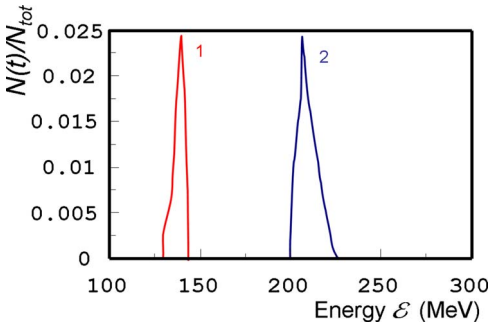


FIG. 6. (Color online) Spectra of protons that are accelerated inside an angle of 10° to the target normal by Gaussian (1) and super-Gaussian (2) pulses.

tion of laser pulse propagation. This cloud generates a longitudinal charge separation electric field [Fig. 4(a)] moving ahead of it and responsible for proton acceleration from the second layer due to repulsion (Coulomb piston) [Fig. 4(b)].

We illustrate the mechanism of proton acceleration as well as the results of the pulse shaping scheme by presenting Fig. 5. In this figure the evolution of total charge [Fig. 5(a)] in the focal spot as well as maximum proton energy is shown along with the evolution of the maximum accelerating longitudinal electric field [Fig. 5(b)] for the cases of Gaussian and flat-top beams. Here the maximum accelerating field is the maximum field that protons experience during the acceleration. The energy curve saturates as the longitudinal field goes to zero, since the acceleration of the second layer of protons is totally due to the moving longitudinal electric field in both cases. One can see that the longitudinal charge separation field as well as the total charge in the case of a flat-top beam is higher; thus the protons are accelerated to higher energies as was theoretically predicted in Sec. III. The effect is due to the fact that flat-top beams evacuate electrons from a larger area on the part of the foil accelerated by the radiation pressure. Moreover, in comparison to the Gaussian beam shape, the flat-top beam more efficiently prevents the electrons from returning to the evacuated region from radial direction due to higher ponderomotive force. That is why the positive charge builds up earlier in the case of flat-top beam as can be seen from Fig. 5(a), while in the Gaussian beam case the positive charge builds up only when the accelerated portion of the foil is separated from the target.

In Fig. 6 we present the spectrum of protons accelerated by a laser pulse with flat-top beam profile along with the spectrum of protons accelerated by the pulse with the Gaussian profile. These protons are contained inside an angle of 10° from the normal to the target. The spectra demonstrate a peaklike behavior. Such a peak formation is typical for Coulomb explosion of a cluster target composed of heavy and light ions [27,28]. There is also a predicted increase in the peak energy from 140 to 210 MeV for a super-Gaussian beam in comparison to the Gaussian beam case. The FWHMs of the high-energy peaks in Fig. 6 are about 5 and 6 MeV, giving $\Delta\mathcal{E}/\mathcal{E}=3.0\%$ for flat-top beam and 3.6% in the Gaussian beam case.

## V. CONCLUSION

In the present paper we found a mechanism of proton acceleration that is different from both the target normal sheath and Coulomb explosion acceleration mechanisms. We showed that the preplasma-free interaction of intense laser pulses with ultrathin double-layer foils in the directed Coulomb explosion regime, which is an effective combination of radiation pressure and Coulomb explosion acceleration mechanisms, allows the production of quasi monoenergetic proton beams remarkable for various applications. In the DCE regime the laser pulse not only expels electrons from the irradiated area but also forces the remaining heavy ions to transform into a cloud expanding predominantly in the direction of laser pulse propagation. This ion cloud generates a longitudinal charge separation electric field moving ahead of it that efficiently accelerates protons from the second layer. We also showed that the use of flat-top beams of the same energy instead of conventional Gaussian beams will lead to the enhancement of the DCE regime through the increase of the Coulomb explosion acceleration stage effect.

However, limits on the experimentally achievable intensity contrast ratio of these laser pulses up to now have prevented such laser-solid dense plasma interactions due to preplasma formation or target destruction before the arrival of the main pulse. It was recently shown [29] that a significant improvement of the laser contrast by three orders of magnitude, yielding a $10^{-11}$ contrast ratio for the Hercules laser system, was achieved, which consequently allows for the preplasma-free interaction of the main pulse with ultrathin foils.

In our 2D PIC simulations of the 500 TW laser pulse preplasma-free interaction with a $0.1\lambda$ aluminum-hydrogen foil we showed that the acceleration of second-layer protons is due to the longitudinal charge separation electric field which moves ahead of the expanding aluminum ion cloud. According to the results of simulations a 500 TW laser pulse is able to produce protons with the energy up to 150 MeV. We also confirmed the analytical prediction that the use of flat-top beams instead of the conventional Gaussian ones, leads a 40% energy gain enhancement over the values generated by the Gaussian beams of the same energy, giving protons with the energy up to 240 MeV. We showed that the effect is due to the fact that flat-top beams evacuate electrons from a larger area on the part of the foil accelerated by the radiation pressure. Moreover, in comparison to the Gaussian beam shape, the flat-top beam more efficiently prevents the electrons from returning to the evacuated region in radial direction due to higher ponderomotive force. That is why the positive charge builds up earlier in the case of the flat-top beam, while in the Gaussian beam case the positive charge builds up only when the accelerated portion of the foil is separated from the target.

## ACKNOWLEDGMENTS

This work was supported by the National Science Foundation through the Frontiers in Optical and Coherent Ultrafast Science Center at the University of Michigan and by Grant No. R21 CA120262-01 from the National Institutes of Health and the International Science and Technology Center (Project No. 2289). The authors would like to thank Dr. T. Zh. Esirkepov for providing the REMP code for the simulations.

[1] A. Maksimchuk, S. Gu, K. Flippo, D. Umstadter, and V. Y. Bychenkov, Phys. Rev. Lett. **84**, 4108 (2000); E. L. Clark, K. Krushelnick, J. R. Davies, M. Zepf, M. Tatarakis, F. N. Beg, A. Machacek, P. A. Norreys, M. I. K. Santala, I. Watts, and A. E. Dangor, *ibid.* **84**, 670 (2000); R. A. Snavely *et al.*, *ibid.* **85**, 2945 (2000).

[2] T. Zh. Esirkepov *et al.*, JETP Lett. **70**, 82 (1999); A. M. Pukhov, Phys. Rev. Lett. **86**, 3562 (2001); Y. Sentoku *et al.*, Appl. Phys. B: Lasers Opt. **74**, 207 (2002); A. J. Mackinnon, Y. Sentoku, P. K. Patel, D. W. Price, S. Hatchett, M. H. Key, C. Andersen, R. Snavely, and R. R. Freeman, Phys. Rev. Lett. **88**, 215006 (2002).

[3] S. V. Bulanov *et al.*, JETP Lett. **71**, 407 (2000); Y. Sentoku *et al.*, Phys. Rev. E **62**, 7271 (2000); H. Ruhl, S. V. Bulanov, T. E. Cowan, T. V. Liseikina, P. Nickles, F. Pegoraro, M. Roth, and W. Sandner, Plasma Phys. Rep. **27**, 411 (2001).

[4] S. V. Bulanov and V. S. Khoroshkov, Plasma Phys. Rep. **28**, 453 (2002).

[5] E. Fourkal *et al.*, Med. Phys. **29**, 2788 (2002).

[6] V. Malka *et al.*, Med. Phys. **31**, 1587 (2005).

[7] M. Roth *et al.*, Phys. Rev. Lett. **86**, 436 (2001).

[8] V. Yu. Bychenkov *et al.*, Plasma Phys. Rep. **27**, 1017 (2001).

[9] A. Macchi, A. Antonicci, S. Atzeni, D. Batani, F. Califano, F. Cornolti, J. J. Honrubia, T. V. Lisseikina, F. Pegoraro, and M. Temporal, Nucl. Fusion **43**, 362 (2003).

[10] M. Borghesi, J. Fuchs, S. V. Bulanov, A. J. Mackinnon, P. K. Patel, and M. Roth, Fusion Sci. Technol. **49**, 412 (2006).

[11] S.-W. Bahk, P. Rousseau, T. A. Planchon, V. Chvykov, G. Kalintchenko, A. Maksimchuk, G. A. Mourou, and V. Yanovsky, Opt. Lett. **29**, 2837 (2004).

[12] V. Yanovsky *et al.*, Opt. Express **16**, 2109 (2008).

[13] J. Koga, T. Zh. Esirkepov, and S. V. Bulanov, Phys. Plasmas **12**, 093106 (2005).

[14] S. C. Wilks *et al.*, Phys. Plasmas **8**, 542 (2001).

[15] S. V. Bulanov, T. Zh. Esirkepov, V. S. Khoroshkov, A. V. Kuznetsov, and F. Pegoraro, Phys. Lett. A **299**, 240 (2002); E. Fourkal, I. Velchev, and C.-M. Ma, Phys. Rev. E **71**, 036412 (2005).

[16] T. Esirkepov, M. Borghesi, S. V. Bulanov, G. Mourou, and T. Tajima, Phys. Rev. Lett. **92**, 175003 (2004).

[17] L. Yin, B. J. Albright, B. M. Hegelich, K. J. Bowers, K. A. Flippo, T. J. T. Kwan, and J. C. Fernandez, Phys. Plasmas **14**, 056706 (2007).

[18] I. Velchev, E. Fourkal, and C.-M. Ma, Phys. Plasmas **14**, 033106 (2007).

[19] T. Zh. Esirkepov *et al.*, Phys. Rev. Lett. **89**, 175003 (2002).

[20] H. Schwoerer, S. Pfotenhauer, O. Jackel, K. U. Amthor, B. Liesfeld, W. Ziegler, R. Sauerbrey, K. W. Ledingham, and T. Esirkepov, Nature (London) **439**, 445 (2006).

[21] V. Yu. Bychenkov and V. F. Kovalev, Quantum Electron. **35**, 1143 (2005).

[22] F. V. Hartemann, *High-Field Electrodynamics* (CRC Press, New York, 2002).

[23] S. S. Bulanov *et al.*, Med. Phys. **35**, 1770 (2008).

[24] E. Gerstner, Nature (London) **446**, 16 (2007); http://eli-laser.eu

[25] R. El-Agmy, H. Bulte, A. H. Greenaway, and D. Reid, Opt. Express **13**, 6085 (2005).

[26] T. Zh. Esirkepov, Comput. Phys. Commun. **135**, 144 (2001).

[27] I. Last, I. Scheck, and J. Jortner, J. Chem. Phys. **107**, 6685 (1997).

[28] I. Last and J. Jortner, Proc. Natl. Acad. Sci. U.S.A. **102**, 1291 (2005).

[29] V. Chvykov, P. Rousseau, S. Reed, G. Kalinchenko, and V. Yanovsky, Opt. Lett. **31**, 1456 (2006).